Langmuir

ARTICLE

pubs.acs.org/Langmuir

Trinuclear Ruthenium Clusters as Bivalent Electrochemical Probes for Ligand−Receptor Binding Interactions

Daniel J. Feld, Hsiao-Tieh Hsu, Amanda L. Eckermann,* and Thomas J. Meade*

Departments of Chemistry, Molecular Biosciences, Neurobiology, Biomedical Engineering and Radiology, Northwestern University, 2145 Sheridan Rd., Evanston, Illinois 60208, United States

Supporting Information

ABSTRACT: Despite their popularity, electrochemical biosensors often suffer from low sensitivity. One possible approach to overcome low sensitivity in protein biosensors is to utilize multivalent ligand−receptor interactions. Controlling the spatial arrangement of ligands on surfaces is another crucial aspect of electrochemical biosensor design. We have synthesized and characterized five biotinylated trinuclear ruthenium clusters as potential new biosensor platforms: $[Ru_3O(OAc)_6CO(4\text{-BMP})(py)]^0$ (**3**), $[Ru_3O(OAc)_6CO(4\text{-BMP})_2]^0$ (**4**), $[Ru_3O(OAc)_6L(4\text{-BMP})(py)]^+$ (**8**), $[Ru_3O(OAc)_6L(4\text{-BMP})_2]^+$ (**9**), and $[Ru_3O(OAc)_6L(py)_2]^+$ (**10**) (OAc = acetate, 4-BMP = biotin aminomethylpyridine, py = pyridine, L = pyC16SH). HABA/avidin assays and isothermal titration calorimetry were used to evaluate the avidin binding properties of **3** and **4**. The binding constants were found to range from $(6.5-8.0) \times 10^6\ M^{-1}$. Intermolecular protein binding of **4** in solution was determined by native gel electrophoresis. QM, MM, and MD calculations show the capability for the bivalent cluster, **4**, to intramolecularly bind to avidin. Electrochemical measurements in solution of **3a** and **4a** show shifts in $E_{1/2}$ of −58 and −53 mV in the presence of avidin, respectively. Self-assembled monolayers formed with **8**−**10** were investigated as a model biosensor system. Diluent/cluster ratio and composition were found to have a significant effect on the ability of avidin to adequately bind to the cluster. Complexes **8** and **10** showed negligible changes in $E_{1/2}$, while complex **9** showed a shift in $E_{1/2}$ of −43 mV upon avidin addition. These results suggest that multivalent interactions can have a positive impact on the sensitivity of electrochemical protein biosensors.

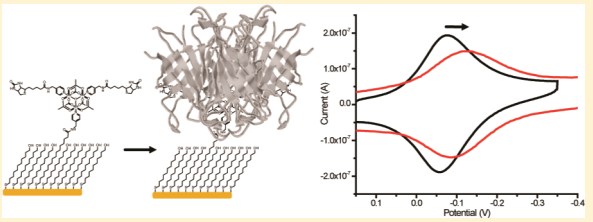

INTRODUCTION

Since the development of the first glucose sensors, electrochemical biosensors have gained popularity due to their low cost, ease of use, and remarkable reproducibility.[1] Electrochemical biosensors have been utilized to detect a variety of biomolecules including DNA, antibodies, enzymes, and proteins.[2−14] Despite their growing popularity, a number of challenges remain in improving sensitivity.[15] Many popular biosensors rely on the measurement of changes in impedance that are caused by target binding to the electrode surface. However, the changes in impedance may be caused by factors unrelated to target binding, such as variations in solution resistance and double layer capacitance. These factors are difficult to analyze without performing a detailed fitting of the data and having a complete understanding of all system components; for example, interactions of the supporting electrolyte with the analyte can alter both solution resistance and double layer capacitance.[16]

A second class of electrochemical protein biosensors rely on a *decrease* in current upon protein binding as the mechanism of sensing.[17−19] Sensors based on this type of negative feedback are not ideal, because current loss (although most often due to protein binding) could be due to degradation of the probe or nonspecific protein binding, leading to an increased number of false positives. Electrochemical biosensors that rely on other mechanisms for detection, such as changes in the redox potential upon protein binding, are, therefore, preferable. Several studies utilize shifts in the redox potential upon protein binding.[8,20] In one such study, a potential shift of approximately 70 mV was observed upon papain binding to a ferrocene−peptide conjugate.[20] In another set of experiments, HIV-1 protease, HIV-1 integrase, and HIV-1 reverse transcriptase binding to a ferrocene−peptide conjugate was monitored by a change in potential of approximately 150 mV.[8] Recently, nanomaterials have been used to enhance the sensitivity of electrochemical biosensors; however, the mechanism of this enhancement is not well understood.[15]

An alternative approach to overcome the obstacle of low sensitivity for protein biosensors is the use of metal complexes that contain multiple protein binding ligands. It has been well-established that multivalent interactions improve binding of small molecules to their target proteins.[21−23] For example, a sialic acid/hemagglutinin conjugate is exploited by influenza viruses to attach to host cells.[21] The potential for fundamentally improving electrochemical biosensors has led us to investigate the effect of monovalent vs bivalent interactions of proteins binding to redox-modified probes.

Received: July 25, 2011
Revised: October 11, 2011
Published: November 04, 2011

Table 1. List of Synthesized Trinuclear Ruthenium Clusters and Their Corresponding Number in This Paper[a]

compound	number
$[Ru_3O(OAc)_6(CO)(MeOH)_2]^0$	**1**
$[Ru_3O(OAc)_6(CO)(4\text{-BMP})(MeOH)]^0$	**2**
$[Ru_3O(OAc)_6(CO)(4\text{-BMP})(py)]^0$	**3**
$[Ru_3O(OAc)_6(H_2O)(4\text{-BMP})(py)]^+$	**3a**
$[Ru_3O(OAc)_6(CO)(4\text{-BMP})_2]^0$	**4**
$[Ru_3O(OAc)_6(H_2O)(4\text{-BMP})_2]^+$	**4a**
$[Ru_3O(OAc)_6(CO)(py)(MeOH)]^0$	**5**
$[Ru_3O(OAc)_6(CO)(4\text{-BMP})(pyC16SH)]^0$	**6**
$[Ru_3O(OAc)_6(H_2O)(4\text{-BMP})(pyC16SH)]^+$	**6a**
$[Ru_3O(OAc)_6(CO)(py)(pyC16SH)]^0$	**7**
$[Ru_3O(OAc)_6(H_2O)(py)(pyC16SH)]^+$	**7a**
$[Ru_3O(OAc)_6(4\text{-BMP})(py)(pyC16SH)]^+$	**8**
$[Ru_3O(OAc)_6(4\text{-BMP})_2(pyC16SH)]^+$	**9**
$[Ru_3O(OAc)_6(py)_2(pyC16SH)]^+$	**10**

[a] Synthetic details are given in the Supporting Information.

The biotin/avidin system was chosen as the model system for this study due to strong noncovalent binding of the host−guest complex ($K_d = 10^{-15}$ M).[24] Avidin has multiple ligand binding sites (tetrameric glycoprotein) and is well-suited for studying the effect of multivalent interactions on protein binding and electron transfer phenomena. In addition, this system is known to be stable to a wide range of pH and temperature.[25] Other studies have been carried out that show the binding affinity of both solubilized and immobilized avidin is not affected during electrochemical experiments.[26−28] The solid-state structure of avidin has been determined crystallographically for a variety of bound substrates, facilitating modeling studies.[6,29−31]

In previous work in our lab, biotinylated iron-cyano and ruthenium-ammine complexes were used as redox modified binding ligands for electrochemical characterization of avidin binding.[13] The current signal in the cyclic voltammograms (CVs) decreased dramatically upon avidin addition and prevented the measurement of electrochemical parameters of the protein-bound species.[13] The protein decreased the coupling between the small, partially buried metal centers and the electrode by insulating the electron transfer process. Slow diffusion of the protein to the electrode further contributes to the signal loss. We have shown spectroscopically that the nonpolar protein should displace outer-sphere water molecules of the metal complex. This reduces the dielectric constant of the surrounding medium, and is hypothesized to affect both the redox potential and the reorganization energy of the complex.[6] Adsorbing iron-cyano complexes onto a monolayer resulted in shifts of −140 mV upon protein binding. However, no electron transfer rate information could be obtained due to low surface coverage and nonspecific nature of the adsorption.[6]

In this work, we describe trinuclear ruthenium clusters as electrochemical probes for ligand−receptor binding (Table 1). These clusters offer several advantages over mononuclear structures. First, the trinuclear ruthenium cluster core was chosen because changes in the environment around one metal center affect the electron transfer properties of other metal centers.[32−44] The clusters are large enough to protrude from the avidin binding site, overcoming the decrease in coupling observed in previous solution-based electrochemical measurements using mononuclear metal complexes. Further, the clusters can be readily incorporated into self-assembled alkanethiol monolayers for biosensor applications that are not inhibited by diffusion.[45−47] Finally, these clusters can be readily modified at all three ruthenium sites, facilitating the investigation of monovalent vs bivalent binding; it becomes unnecessary to synthesize ligands containing two biotin moieties when using the trinuclear ruthenium cluster-based system.

We have synthesized a series of five biotinylated trinuclear ruthenium clusters as shown in Schemes 1 and 2. These clusters were designed to study the effect of monovalent vs bivalent interactions on both protein binding and electron transfer reactions. The ability of **3** and **4** to bind to avidin was analyzed using 4′-hydroxyazobenzene-2-carboxylic acid (HABA) assays. Isothermal titration calorimetry was performed using **3** and **4** to determine binding constants of the complexes with avidin. Native gel electrophoresis was used to determine the mechanism of avidin binding of **4**. Modeling was performed for **4** to ascertain the possibility of this cluster intramolecularly binding two protomers of avidin simultaneously. Finally, electrochemistry of **3** and **4** in solution, and **8**−**10** with self-assembled monolayers, was performed to investigate the effect of monovalent vs bivalent interactions on electron transfer for these two systems.

EXPERIMENTAL SECTION

Materials and Methods. $RuCl_3 \cdot xH_2O$ was purchased from Strem Chemicals (Newburyport, MA) and used without further purification. Carbon monoxide was purchased from Matheson Tri-Gas. Dimethylformamide, chloroform, and methanol were purified on a column of activated alumina under argon. Gold wire was purchased from Alfa Aesar (Ward Hill, MA). Nanopure water was obtained using a Millipore Q-Guard system equipped with a quantum Ex cartridge (Billerica, MA). 4-Aminomethylpyridine was purchased from Sigma-Aldrich Chemical Co. (St. Louis, MO) and was distilled prior to use. All other reagents were purchased from Sigma-Aldrich Chemical Co. (St. Louis, MO) and were used without further purification. Mass spectra were obtained on a Varian 1200L single-quadrupole electrospray mass spectrometer. NMR spectra were obtained either on a Varian INOVA spectrometer (500 MHz) or a Bruker Avance III spectrometer (500 MHz). UV−visible absorption spectra were obtained on an Agilent 8453 spectrophotometer (Foster City, CA). All measurements were carried out using a quartz cuvette at room temperature. Electrochemical measurements were performed in 150 mM pH 7 phosphate buffer containing 100 mM NaCl using a CH Instruments 660A workstation and a standard cell with three electrodes (gold working electrode, platinum wire counter electrode, and Ag/AgCl reference electrode).

HABA/Avidin Assays. HABA/avidin reagent was purchased from Sigma-Aldrich and was reconstituted with 10 mL water. The assay was conducted according to the instructions provided by Sigma-Aldrich. Details are provided in the Supporting Information.

Isothermal Titration Calorimetry. Isothermal titration calorimetry (ITC) was performed using a MicroCal iTC_{200} calorimeter (Northampton, MA). For a typical experiment, the sample cell contained 240 μL of a 6 μM avidin solution (24 μM protomer) in 150 mM potassium phosphate buffer. The injection syringe was filled with 40 μL of a 300 μM solution of the monobiotinylated cluster **3** and a 150 μM solution of the bis-biotinylated cluster **4** in the same buffer. The solutions of the ruthenium clusters were injected into the sample cell in 1.5 μL aliquots every 120 s until saturation was observed. Data were fit in *Origin 7.0* using the One Sites Model to obtain enthalpies (ΔH), entropies (ΔS), and binding constants (K_a).

Scheme 1. Clusters Synthesized for Experiments in Solution[a]

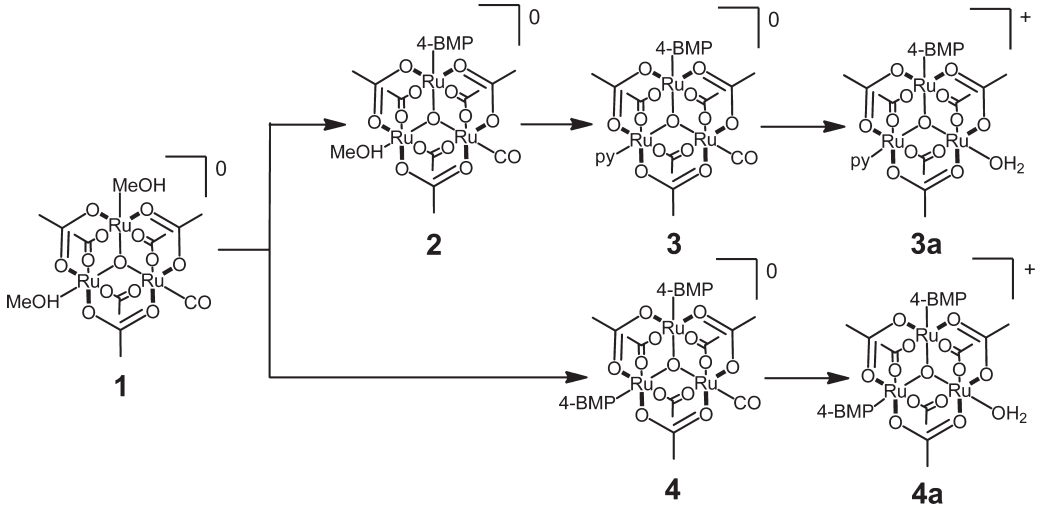

[a] Synthetic details are given in the Supporting Information.

Scheme 2. Clusters Synthesized for Monolayer Experiments[a]

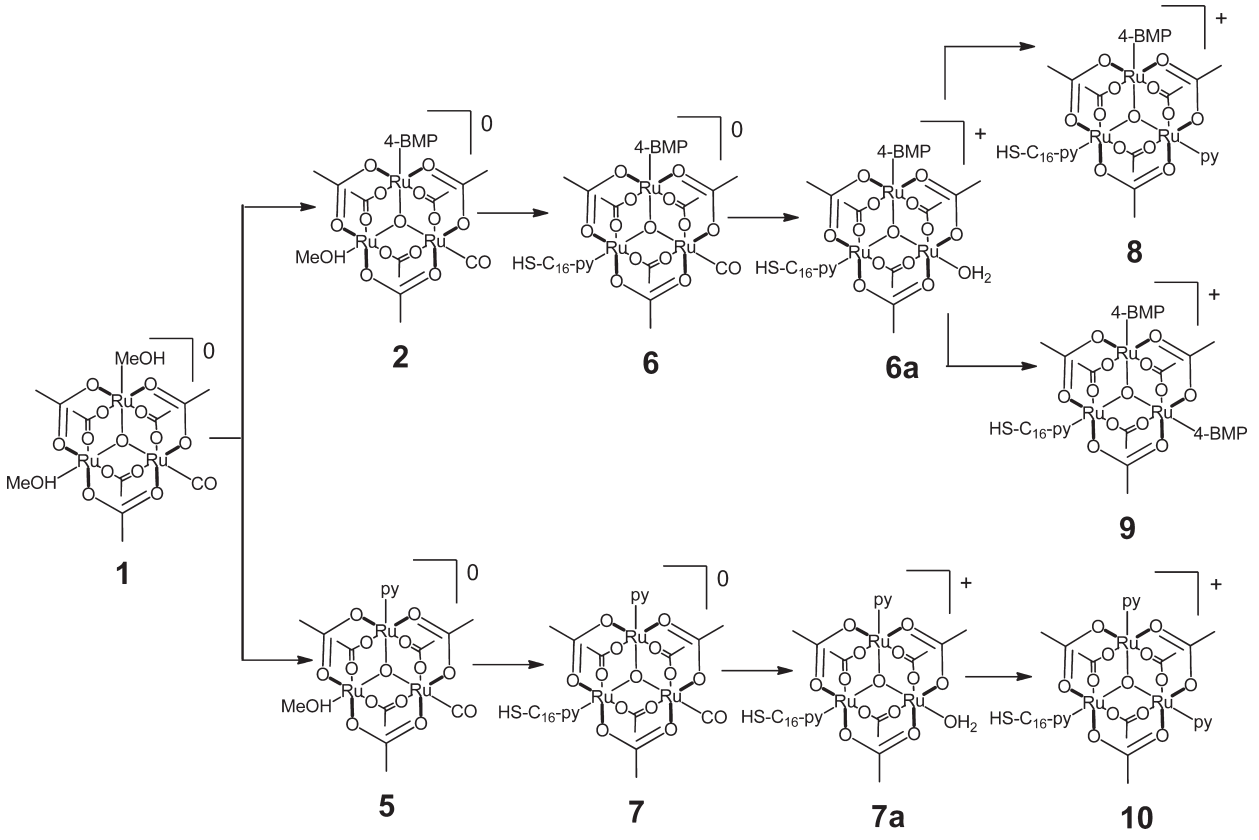

[a] Synthetic details are given in the Supporting Information.

Native Gel Electrophoresis. Native gel electrophoresis was performed based on a procedure described by Gallagher.[48] A 1 mm gel containing 5% acrylamide was prepared by combining 3.3 mL of 30% acrylamide/0.8% bisacrylamide, 12.7 mL of water, and 4.0 mL of 400 mM sodium phosphate buffer (pH 7.0). Polymerization was initiated by the addition of 50 μL of 10% (w/v) ammonium persulfate and 10 μL of *N,N,N′,N′*-tetramethylethylenediamine (TEMED). The gel was allowed to polymerize overnight. Four solutions of avidin (5 mg/mL) were prepared in 100 mM sodium phosphate buffer (pH 7.0). Four equivalents of either **3** or biotin or two equivalents of **4** were added to a protein solution and incubated overnight at room temperature. 80% glycerol was then added to each solution to a total glycerol concentration

dx.doi.org/10.1021/la202882k |*Langmuir* 2012, 28, 939–949

(v/v) of 5%. Five microliters of each solution was loaded onto the gel. Electrophoresis was performed toward the cathode in 100 mM sodium phosphate buffer (pH 7.0) at a constant voltage of 80 V for 6 h at room temperature using a Bio-Rad PowerPac 300 power supply in a Bio-Rad Mini-Protean Tetra Cell. After electrophoresis, the gel was rinsed with water and stained with Bio-Rad Bio-Safe Coomassie G-250 stain.

Monolayer Preparation. For self-assembled monolayer studies, the working electrode was prepared by cutting a 6.5 cm length of 99.99% gold wire (0.127 mm diameter, Alfa Aesar Premion). Two centimeters of the wire was melted into a sphere using a Bunsen burner. Digital microcalipers were used to measure the diameter of the sphere for calculation of the electrode surface area. The spherical electrode was electrochemically cleaned using dilute H_2SO_4, cycling the potential from 0 to 1.6 V until a constant current was observed. Following this cleaning procedure, the electrode was rinsed with water and EtOH before being submerged in the monolayer deposition solution.

Monolayers with clusters **8**−**10** were prepared as follows. Gold ball electrodes were soaked in 5:1, 10:1, 20:1, and 40:1 diluent/cluster solution in EtOH (2 mM total thiol) overnight. The diluent was either $HO(CH_2)_{11}SH$ or $HO(CH_2)_{16}SH$. The cluster was either **6** or **7**. Monolayers were rinsed copiously with EtOH followed by H_2O. The clusters on the monolayers were then electrochemically oxidized by repeatedly cycling the potential between −0.6 and 0.8 V (vs Ag/AgCl) at 200 mV/s. Upon oxidation, the CO ligand of **6** and **7** becomes labile and is replaced by H_2O, forming the aquo clusters **6a** and **7a**.[45−47] The reaction was monitored by a decrease in the current of **6** or **7** at $E_{1/2}$ ∼650 mV and an increase in the current of **6a** and **7a** at $E_{1/2}$ ∼ −100 mV. The process was determined to be complete when constant current was observed for **6a** and **7a** (typically no longer than 30 min). An example cyclic voltammogram for this procedure is presented in SI Figure S15. The gold ball electrodes were then submerged in either 1 mM 4-BMP or pyridine (in H_2O) for 24 h to form the desired species **8**−**10**.

Electrochemical Methods. Electrochemical experiments were performed using a standard three-electrode setup with a Pt wire counter electrode and a Ag/AgCl reference electrode. All potentials are reported in reference to the Ag/AgCl electrode. All samples were purged with nitrogen prior to performing electrochemical experiments. For solution studies using the ruthenium clusters **3** and **4**, a gold disk working electrode was used. Prior to the solution experiments, the working electrode was polished on 0.05 μm alumina and electrochemically cleaned using dilute H_2SO_4, cycling the potential from 0 to 1.6 V until a constant current was observed. In a typical experiment, measurements were performed using 0.4 mM cluster in pH 7.0 PBS buffer containing 100 mM NaCl. Using a procedure similar to that described in the previous section, potentials were cycled between −0.4 and 0.8 V (with stirring) to oxidize the cluster, making the CO labile.[49] This was done until a constant current was observed for the newly formed aquo species **3a** and **4a**. The typical reaction took several hours to complete in solution. Avidin binding studies were performed on the resulting aquo complexes. Cyclic voltammetry was performed for a series of scan rates ranging from 10 mV/s to 10 000 mV/s. CH Instruments 660A software was used to determine $E_{1/2}$ and peak currents. $E_{1/2}$ is defined as $(E_{pc} + E_{pa})/2$. The clusters were incubated with an excess of avidin for 1 h. Cyclic voltammetric measurements were then repeated for the same series of scan rates.

For electrochemical experiments using monolayers of **8**−**10**, cyclic voltammetric measurements were performed in pH 7.0 PBS buffer containing 100 mM NaCl. For each diluent/cluster ratio, cyclic voltammetry was performed employing a series of scan rates. For monolayers with a C16 diluent, scan rates from 0.001 V/s to 100 V/s were performed. For monolayers with a C11 diluent, scan rates from 0.01 V/s to 2500 V/s were performed. Tafel plots were generated as described elsewhere in order to determine electron transfer rate parameters.[4] To determine the uncompensated solution resistance, alternating current impedance measurements were performed. After the initial electrochemical experiments, the electrodes were submerged in a 30 μM avidin solution at 37 °C overnight to maximize protein binding to the cluster. After avidin binding, the electrochemical experiments were repeated, and Tafel plots were generated to determine electron transfer rate parameters.

Modeling. *Quantum Mechanical (QM) and Molecular Mechanical (MM) Calculations.* The $[Ru_3O(OAc)_6(CO)(4\text{-BMP})_2]^0$ cluster was constructed by modifying the available crystal structure of $[Ru_3O(OAc)_6(CO)(mbpy)_2]^{2+}$ (mbpy = *N*-methyl-4,4′-dimethylbipyridinium ion) and appending the biotin arms.[50] In order to evaluate the atomic charges and the force constants, a quantum mechanical (QM) calculation was carried out to optimize the geometry of the cluster. Calculations were performed using the *Jaguar 7.7* package implemented in *Schrodinger 9.1*.[51] DFT calculations were performed with the B3LYP hybrid functional together with the 6-31++G** basis set for all atoms except the ruthenium.[52,53] Ruthenium atoms were treated with an ECP basis of TVZ quality, splitting off the most diffuse s, p, and d primitive in the standard LANL2DZ contraction.[54,55] The cluster geometry was fully optimized and the CHelpG charges were calculated using a radius of 2.34 Å for ruthenium.[56]

All the force field calculations were performed in *MacroModel 9.8* using the OPLS2005 force field. The bonding between the metal and the ligand was established using the method proposed by Brandt et al.[54] The bond, angle, torsional, and other parameters were obtained by using standard Norrby Liljefors techniques.[57]

Docking of the Cluster to Biotin Binding Sites in Avidin. The dimeric biotin-bound crystal structure of avidin (1AVD.pdb) was obtained from the Research Collaboratory for Structural Bioinformatics Protein Data Bank and was used for the docking studies.[58] The Crysin crystallographic tool implemented in the Sybyl interface was utilized to generate the tetramer using appropriate unit cell parameters obtained from the crystallographic data.[59] Of the four monomers of the avidin tetramer, the two monomers with similar orientations of the biotin binding pocket (i.e., adjacent monomers between which the trinuclear ruthenium cluster could act as a bridge between binding sites) were selected for the docking study.

The FlexiDock docking tool for protein/ligand pairs in the Sybyl interface was used for docking of the ruthenium cluster into the biotin binding sites of the two avidin monomers.[59] FlexiDock works in torsional space, keeping the bond lengths and angles constant while allowing the amino acid residues that interact with the ligand to be flexible during the docking process. Using a genetic algorithm (GA), FlexiDock generated many different docked poses for the $[Ru_3O(OAc)_6(CO)(4\text{-BMP})_2]^0$ cluster. Three minimum energy conformations of the cluster with avidin were selected for further study.

Molecular Dynamics (MD) Simulations. Molecular dynamics (MD) simulations were carried out using the three minimum energy conformations of **4** with avidin (generated from docking studies) using the modified OPLS2005 force field in *MacroModel 9.8*.[60] The OPLS2005 force field was modified by incorporating new atom type, vdw type, and polarities of bonds. The earlier computed stretch, bend, and torsion parameters (from QM) were used and the corresponding files were modified. In the *MacroModel* dynamic panel, stochastic dynamics were chosen as it includes random forces that simulate the buffering of a system by solvent molecules. To constrain the bond lengths to the original value, the SHAKE option was selected. The simulations were carried out for all the complexes of **4** with avidin at 300 K with a time step of 1.5 fs and equilibration time of 1 ps. MD simulations were run for 5 ns, recording the energy and trajectory information. Out of the three minimum energy conformations generated from docking studies, only one showed all the critical interactions of biotin with the ligand binding domain of avidin (Figure 1). System equilibrium was reached within 5 ns (SI Figure S1).

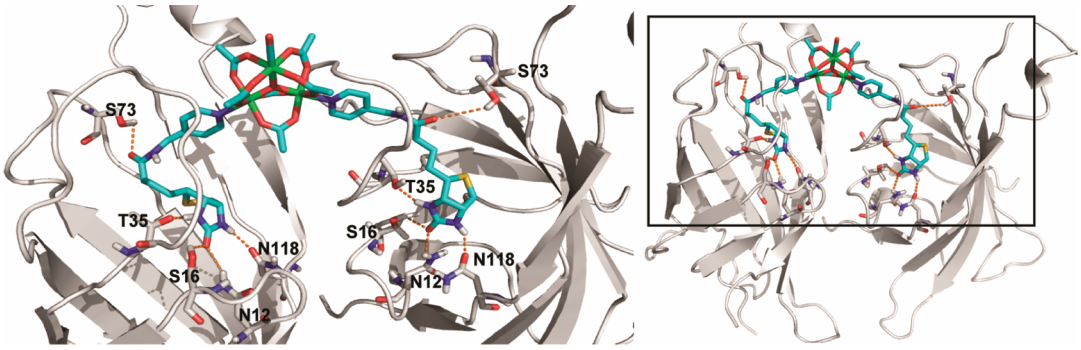

Figure 1. Energy minimized structure of **4** intramolecularly bound to two adjacent protomers of avidin. The A and D subunits are shown. All critical hydrogen bond interactions between the biotin moieties and avidin are maintained (left).

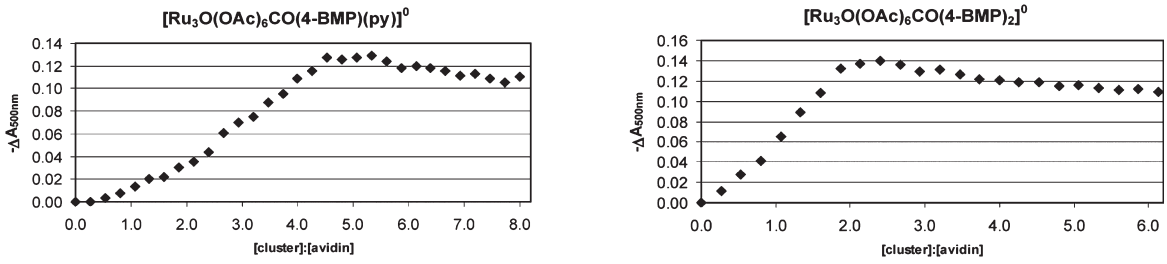

Figure 2. Absorption titration curves from HABA/avidin assays of **3** (left) and **4** (right). The equivalence points of 4.5 for **3** and 2.1 for **4** are close to the expected values indicating that the trinuclear ruthenium clusters bind to avidin.

RESULTS AND DISCUSSION

Clusters of the formula $[Ru_3O(OAc)_6(CO)LL']$ were successfully synthesized, where L, L′ = pyridine, 4-BMP, or pyC16SH (Schemes 1 and 2). These intermediate CO complexes facilitate the purification of the clusters by minimizing the number of products that can be generated. Simplifying the mixture resulting from direct substitution of pyridine onto the cluster ultimately results in higher yields. The CO complexes **3** and **4** were subsequently electrochemically converted to aquo complexes for solution measurements of avidin binding. The CO complexes **6** and **7** were used to form self-assembled monolayers on gold and subsequently electrochemically converted to aquo species **6a** and **7a**. **6a** and **7a** were then reacted with pyridine or 4-BMP to form **8**−**10** for monolayer studies of avidin binding.

HABA/Avidin Assays. Upon addition of **3** and **4** to the HABA/avidin solution, the absorbance at 500 nm was observed to decrease. This behavior indicates that these complexes displace HABA (4-hydroxyazobenzene-2-carboxylic acid, $K_d = 5 \times 10^{-6}$ M) and bind to avidin in its place.[61,62] Figure 2 shows the absorption titration curves for **3** and **4**.

According to the plot for **3**, the equivalence point is approximately 4.5 biotin molecules per avidin. Theoretically, the equivalence point should be 4.0, as avidin is tetrameric, and **3** contains a single biotin moiety. An equivalence point of 4.5 suggests that **3** binds to avidin with an affinity similar to that of HABA (Figure 2). A slight excess of the biotinylated cluster must be added to the solution to shift the equilibrium enough so that all of the HABA becomes displaced in favor of the trinuclear ruthenium cluster. Steric hindrance is one possible reason for **3** having a binding affinity similar to that of HABA. If 4 equiv of **3** binds to avidin, two clusters must be brought within close proximity to each other for binding to occur in two adjacent binding pockets of the same protein.

The absorption titration curve for **4** shows an equivalence point of 2.1 biotin molecules per avidin. Since **4** is bivalent, the theoretical equivalence point is 2.0, assuming that the two biotin moieties are far enough apart to bind two protomers of avidin simultaneously. This type of bivalent binding could occur two ways: (i) intramolecular binding between two sites of the same protein or (ii) intermolecular binding between protomers on two different proteins. Previous work by Green and co-workers has shown that, with 23 methylene bond lengths between the acid carbonyls of a bivalent biotinylated compound, intramolecular binding occurs. In addition, when there are 12 methylene bond lengths between the acid carbonyls, intermolecular binding between protomers on two different proteins occurs.[63,64] The distance between the two biotin acid carbonyls in **4** is approximately the equivalent of 16 methylene bond lengths. This value lies in between the two systems studied by Green and co-workers for intra- vs intermolecular binding. Based only on this comparison, it is unclear if inter- or intramolecular binding is occurring in our bivalent system. To further investigate the avidin binding properties of **3** and **4**, isothermal titration calorimetry was performed to determine the binding constants, as well as ΔG, ΔH, and ΔS.

Isothermal Titration Calorimetry. Isothermal titration calorimetry (ITC) of **3** and **4** was used to determine the binding constants and other thermodynamic parameters of avidin binding. Data were fit in *Origin 7.0*, and the best fits for all data were obtained using the One Sites Model. Results are summarized in Table 2. Representative ITC data are shown in SI Figures S2−S4.

Biotin is known to bind to avidin with a binding constant of 10^{15} M^{-1}.[24] For a more accurate comparison of our cluster binding constants to avidin, ITC was performed for the ligand 4-BMP. As has been previously shown, conversion of the terminal acid of biotin to an amide decreases the binding affinity

dx.doi.org/10.1021/la202882k |*Langmuir* 2012, 28, 939–949

Table 2. Isothermal Titration Calorimetry Data of Avidin Binding to 3 and 4 at 25 °C

compound	K (M^{-1})	ΔG (kcal/mol)[a]	ΔH (kcal/mol)	ΔS (cal/mol/deg)
4-BMP	1.1×10^8	−11.0	−16.7	−19.2
$[Ru_3O(OAc)_6(CO)(4\text{-BMP})(py)]^0$	8.0×10^6	−9.5	−8.1	4.6
$[Ru_3O(OAc)_6(CO)(4\text{-BMP})_2]^0$	6.5×10^6	−9.3	−18.0	−29.2

[a] Calculated from ΔH and ΔS at 298 K.

by approximately 7 orders of magnitude.[65] The binding constant for **3** was found to be 8.0×10^6 M^{-1}, a little more than 1 order of magnitude smaller than 4-BMP. This result is not surprising given the increased steric bulk of the large trinuclear ruthenium cluster as compared to 4-BMP alone. In addition, once one cluster is bound, it may be possible for the pyridine ligand of **3** to partially block access of the nearby binding pocket to another ligand, further decreasing the ability of a second cluster to bind in the adjacent binding site. Notably, the binding constants reported by Barker et al. for biotinylated iron(II) tetracyano complexes with avidin are smaller than the binding constant observed here for 4-BMP, but larger than that for **3**.[6] This trend is as expected since the mononuclear complexes analyzed by Barker et al. are more sterically hindered than 4-BMP, but less sterically hindered than **3**.

The binding constant for **4** was observed to be similar to, but slightly less than **3**, despite having two binding ligands. For an intramolecular binding mechanism, one possible explanation is that, after the first biotin of the cluster binds in one binding site, it is sterically inhibited for the second biotin and the protein to adopt the conformations needed for binding to the adjacent protomer. For an intermolecular binding mechanism, the steric hindrance encountered by two proteins being forced into close proximity with each other would be the likely cause for the observation of a smaller binding constant for **4** as compared to **3**.

For all compounds studied, binding to avidin was exothermic. The largest enthalpy was observed for the bivalent cluster **4**. It is energetically more favorable for the hydrophobic biotin moieties to be bound in the hydrophobic pocket of avidin than to be in aqueous solution. The smaller enthalpy observed for **3** is likely due to it being energetically unfavorable to have two large trinuclear ruthenium clusters in close proximity to one another when they are bound to two adjacent protomers.

Binding is entropically favorable for the monovalent cluster **3**; however, the binding of the bivalent cluster **4** is *not* an entropically favorable process. It is known that protein binding involves processes that both increase and decrease the entropy of the system.[66,67] The loss of water from the binding pocket of the protein increases entropy (desolvation entropy). The loss in rotational degrees of freedom for the binding ligand decreases entropy (conformational entropy).[66,67] The total desolvation entropy should be similar for both complexes. When **3** binds to avidin, there is a loss of conformational entropy for the biotin moieties of the cluster. However, although somewhat sterically hindered, the metal cluster portion of the complex is still free to rotate, resulting in larger conformational entropy. The large, monovalent cluster may additionally disrupt the structure of the protein distal to the binding site, increasing conformational entropy of the protein. These two phenomena overcome the loss in conformational entropy for the biotin moieties of the complex upon protein binding. Consequently, for **3**, the loss of conformational entropy is less than the desolvation entropy resulting in an overall increase in entropy (favorable) upon binding.

For the bivalent cluster, **4**, binding both biotin moieties at the same time restricts the conformational degrees of freedom available to the metal portion of the cluster. If intramolecular binding is occurring, the structure of the protein distal to the binding site will not be as disrupted as for monovalent cluster binding. Therefore, for the bivalent system, the unfavorable loss of conformational entropy is more than the desolvation entropy, resulting in an overall decrease in entropy (unfavorable) upon binding.

Both the enthalpy and entropy contribute to the overall Gibbs free energy of binding. As is often the case at room temperature, the enthalpy contributes more than the entropy to the overall Gibbs free energy change associated with protein binding. It is no surprise that for a biotin/avidin-based system there is a large driving force for binding; thus, all binding events are spontaneous at room temperature. Somewhat surprising, however, is that, due to the entropic contribution, the bivalent cluster, **4**, has a smaller driving force for binding than the corresponding monovalent cluster, **3**. Given this unexpected result, native gel electrophoresis was performed to further determine the mechanism of binding of **4** to avidin in solution.

Native Gel Electrophoresis. Native gel electrophoresis was performed to determine the mechanism of binding of the bivalent cluster, **4**, to avidin in solution. This technique is dependent upon both the protein charge and size. Addition of the neutral cluster will not change the charge and, relative to the size of the avidin tetramer, the size of the protein complex will not differ significantly. Thus, the migration of a complex of **3** with avidin is not expected to differ significantly from the migration of native avidin. If intramolecular binding is the predominant mechanism, a complex of **4** with avidin should migrate at the same rate as native avidin and a complex of **3** with avidin. If intermolecular binding is the predominant mechanism, a complex of **4** with avidin should migrate more slowly than native avidin and a complex of **3** with avidin.

As expected, the mobility of a conjugate of **3** with avidin was the same as that of native avidin. However, native gel electrophoresis showed that the mobility of a conjugate of **4** with avidin was less than that of native avidin (see SI Figure S5). This result indicates that, under the conditions of this experiment, intermolecular binding predominates in solution, where multiple proteins are linked together by the bivalent cluster. Given these results, QM, MM, and MD calculations were carried out for **4** to better understand the possibility of intramolecular binding of the bivalent cluster to avidin in cases where intermolecular binding is prevented. Of particular interest is how intramolecular binding may be favored on a monolayer with a low cluster concentration.

Modeling. QM, MM, and MD calculations show that complex **4** is capable of binding to two adjacent protomers of avidin as shown in Figure 1. The biotin moieties bind to the expected binding sites in both protomers as previously characterized.[31] The 4-BMP ligands are stabilized by several hydrogen bonding pairs that are observed in native avidin−biotin. Namely, hydrogen

Table 3. Solution Electrochemical Data before and after Avidin Binding[a]

compound	$E_{1/2}$ (mV)	$E_{1/2}$ with avidin (mV)	$\Delta E_{1/2}$ (mV)
$[Ru_3O(OAc)_6(H_2O)(4\text{-BMP})(py)]^+$	−54	−112	−58
$[Ru_3O(OAc)_6(H_2O)(4\text{-BMP})_2]^+$	−32	−85	−53

[a] Potentials are reported vs Ag/AgCl at a scan rate of 500 mV/s.

bonds are observed between the ureido ring of biotin and N12, S16, Y33, T35, T77, and N118 of avidin. S73 and S75 bond with the carbonyl of the amide bond.

While several biotinylated-transition metal complexes have been synthesized, only three others have been structurally characterized bound to avidin, two of these by crystallographic analysis.[6,68−70] The majority of the bound trinuclear ruthenium cluster lies near a hydrophilic portion of the protein while a smaller portion of it is exposed to the hydrophobic part of the protein surface bridging between two avidin protomers. Our model further shows there is no major reorganization of the avidin backbone to accommodate the intramolecularly bound cluster, indicating that this type of binding should be stable. We hypothesized that the changing environment around the trinuclear ruthenium cluster after protein binding would have an observable effect on the electrochemical properties of **4** bound to avidin.

Solution Electrochemistry. In previous work using small, mononuclear metal complexes, a significant loss in current was observed in cyclic voltammograms after avidin binding.[13] A decrease in electronic coupling due to the insulating properties of the protein was determined to be one of the causes for this phenomenon. It was hypothesized that coupling with the electrode (and therefore the observed current) could be improved by using larger, trinuclear ruthenium clusters as electrochemical probes. These species would allow us to see changes in electrochemical parameters upon avidin binding, caused by the different environment surrounding the metal complex. Specifically, the nonpolar protein should displace water molecules from the cluster, reducing the dielectric constant of the surrounding medium, affecting both the redox potential and the reorganization energy of the cluster.

For each experiment, approximately 0.4 mM solutions of **3** and **4** in pH 7 PBS were used. First, these complexes were electrochemically converted, through loss of the CO moiety, to the aquo species **3a** and **4a** as described in the Experimental Section. The cyclic voltammetry (CV) data for **3a** and **4a** are summarized in Table 3 and a representative voltammogram is shown in Figure 3. The observed $E_{1/2}$ values are similar to those reported in the literature for similar trinuclear ruthenium clusters.[44,50,71−78] ΔE_p ($E_a - E_c$) was observed to be, on average, 65 mV for each cluster studied, indicative of a reversible electrochemical couple.[79] The current ratio of (i_a/i_c) was typically approximately 0.7.

After performing cyclic voltammetry for a series of scan rates to ensure a well-behaved system, excess avidin was added to the solution. Binding was allowed to occur for 1 h. After avidin addition, cyclic voltammetric experiments were repeated. As was observed in previous experiments using $[Ru(NH_3)_5(4\text{-BMP})]^{2+}$ and $[Ru(NH_3)_5(4\text{-DMP})]^{2+}$, a decrease in current was observed (Figure 3).[13] However, unlike our previously reported examples, the current signal did not entirely diminish. Using trinuclear ruthenium clusters, we achieved the goal of maintaining coupling

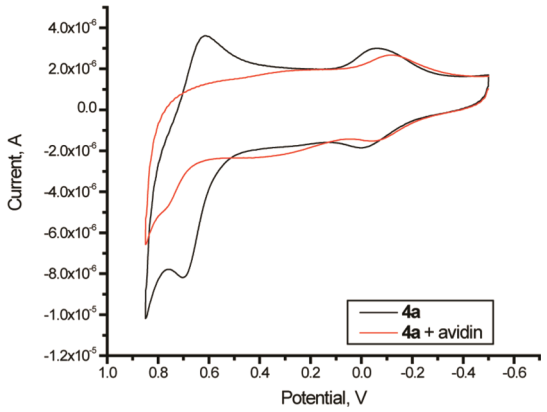

Figure 3. Solution CV data for **4** (black). Upon oxidation, the carbonyl is lost from **4** ($E_{1/2} \sim 650$ mV) and **4a** is formed ($E_{1/2} \sim -100$ mV). Upon avidin addition (red), a shift in $E_{1/2}$ of −53 mV is observed along with a slight decrease in current.

with the electrode after avidin binding, allowing electrochemical measurements to be made upon protein binding.

Reversible electrochemistry was observed for **3a** and **4a** after avidin binding with i_a/i_c of 1.1 and 0.9, respectively. ΔE_p was observed to be 64 mV and 73 mV. Shifts in $E_{1/2}$ upon protein binding are summarized in Table 3. $E_{1/2}$ of **3a** was found to shift −58 mV, and $E_{1/2}$ of **4a** was observed to shift −53 mV. The negative direction of each shift indicates that the oxidized form of the cluster is more stable when bound to avidin.[6] It is possible that this is due to the ruthenium cluster portion of these complexes sitting near a hydrophilic portion of avidin. The similarity of the shifts for the monovalent and bivalent systems is likely due to the intermolecular protein binding mechanism observed in solution. Given this mechanism, it is unlikely that the monovalent and bivalent clusters experience significantly different environments from each other when bound to the protein. To investigate a system in which intermolecular binding is less likely and diffusion limitations are removed, experiments were performed with the clusters incorporated into a self-assembled monolayer.

Monolayer Electrochemistry. In addition to decreased electronic coupling, a second possible reason for the significant decrease in current upon protein binding as observed in previous work is slow diffusion of the protein to and from the electrode.[13] A system in which the metal complex is covalently attached to an alkanethiol monolayer can overcome these diffusion limitations. Determination of the electron transfer rate is facilitated by avoiding diffusion limitations. We expected to see a difference in shifts of $E_{1/2}$ upon protein binding for the monovalent and bivalent systems. This difference would be caused by the possibility of intramolecular binding for the bivalent system due to spatial and diffusion limitations preventing intermolecular binding for the surface-confined cluster at low cluster surface concentrations. Furthermore, the different environment surrounding the metal complex upon protein binding was expected to change the rate of electron transfer.

Clusters **8**−**10** were generated on the monolayer from **6** and **7** using cyclic voltammetry to form **6a** and **7a**. This process was followed by soaking the monolayer in a 1 mM solution of pyridine or 4-BMP to attach the desired ligand, forming **8**−**10** (Scheme 3).[45−47] For all systems studied, the plot of i_p vs scan rate of the CV data was linear, as expected for the electrochemistry of a redox species on a

dx.doi.org/10.1021/la202882k |*Langmuir* 2012, 28, 939–949

Scheme 3. Electrochemical Oxidation of 6 in a $HO(CH_2)_{11}SH$ Monolayer to Synthesize 9[a]

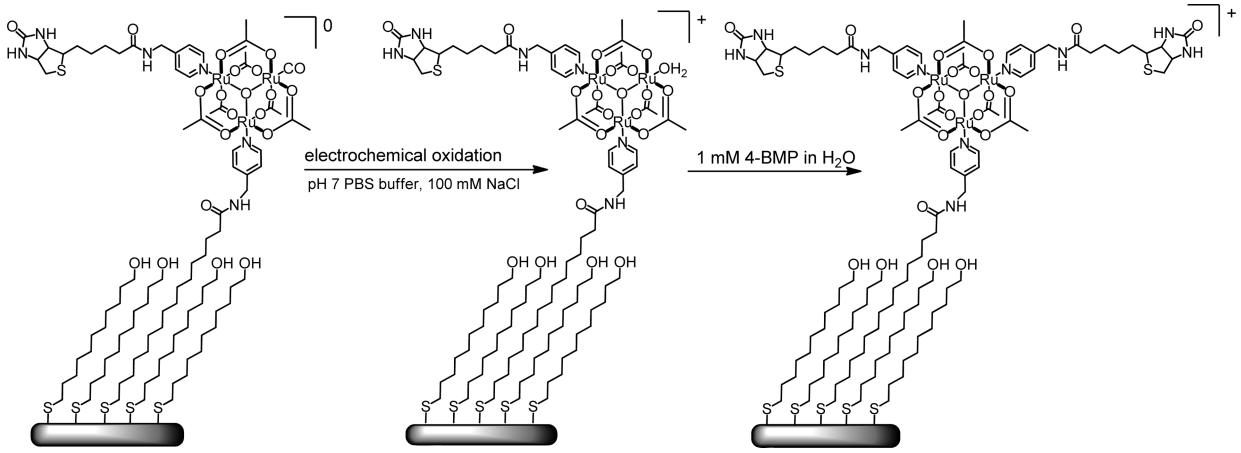

[a] Upon oxidation, the CO of **6** becomes labile and is replaced by a solvent molecule to form **6a**. Submerging the monolayer in a solution containing 4-BMP allows for the synthesis of **9**.

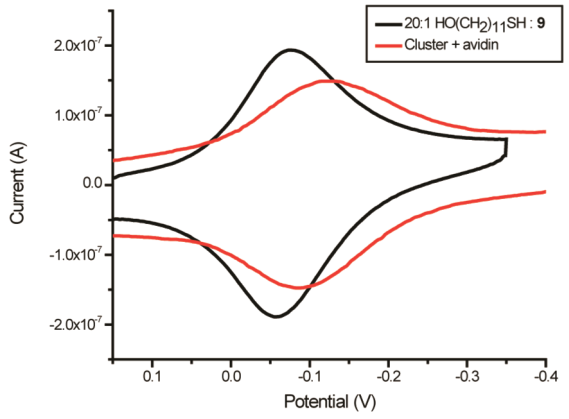

Figure 4. Ratio of 20:1 diluent $HO(CH_2)_{11}SH$ to cluster **9** allows for adequate protein binding to the surface of the monolayer. This binding event is evidenced by a shift of −43 mV from the original monolayer (black) after avidin addition (red).

monolayer. Therefore, it can be inferred that the monolayers are well-packed (SI Figure S7−S14).[4] In addition, at low scan rates, the anodic and cathodic peak separation, ΔE_p, is small, <15 mV, as expected for a well-behaved monolayer.[4,80] $E_{1/2}$ values of the trinuclear ruthenium clusters were similar to those observed for analogous complexes reported in the literature.[44,50,71−78] A representative CV is shown in Figure 4 for the bivalent cluster, **9**.

The ratio of diluent hydroxyalkanethiol to cluster-alkanethiol was found to have a significant impact on protein binding at the monolayer surface. Using **9** and a C16 diluent, a series of monolayers with varying diluent/cluster concentrations (5:1, 10:1, 20:1, and 40:1) was tested. As shown in Table 4, in general, as the diluent/cluster ratio increased, the change in the observed $E_{1/2}$ upon protein binding increased. The shift in $E_{1/2}$ observed for the 5:1 ratio was −11 mV compared with −23 mV for the 20:1 ratio. The shifts in $E_{1/2}$ observed for both the 20:1 and 40:1 ratios were the same within experimental error. This result is indicative of a greater percentage of the clusters on the surface being bound by avidin for monolayers containing a higher percentage of diluent hydoxyalkanethiol. Based on these results, we hypothesize that, if the cluster concentration on the monolayer is too high, steric

Table 4. Electrochemical Data for a Monolayer Cluster Concentration Study Using $[Ru_3O(OAc)_6(4\text{-BMP})_2(4\text{-AMP-CO}(CH_2)_{15}SH)]^{+}$[a]

ratio of diluent to cluster	$E_{1/2}$ (mV)	$E_{1/2}$ with avidin (mV)	$\Delta E_{1/2}$ (mV)	k_{ET} (s^{-1})
5:1 C16/C16	−50	−62	−11	0.3
10:1 C16/C16	−46	−46	0	0.4
20:1 C16/C16	−39	−62	−23	0.4
40:1 C16/C16	−58	−81	−23	0.3
10:1 C11/C16	−67	−95	−28	60
20:1 C11/C16	−65	−108	−43	75

[a] Potentials are reported vs Ag/AgCl.

interactions between proteins would prevent each cluster on the surface from binding to avidin.[81−83] This crowding of protein on the surface of the monolayer would result in smaller observable changes in ET parameters, as many of the clusters remain unbound. In light of these results, in order to maximize the signal-to-noise ratio between the faradaic and nonfaradaic currents while at the same time maximizing the changes in electrochemical parameters upon protein binding, a 20:1 diluent/cluster ratio was chosen for all subsequent experiments.

Based on literature, we hypothesized that using a diluent alkanethiol the same length as that attached to the trinuclear ruthenium cluster may hinder avidin from binding strongly to the clusters on the surface due to steric interactions with the monolayer in the third dimension.[84] To test this hypothesis, a shorter, C11 diluent hydroxyalkanethiol was used to prepare the monolayer. Using a 20:1 diluent/cluster ratio to form the monolayer incorporating $HO(CH_2)_{11}SH$ as the diluent, a shift in $E_{1/2}$ of −43 mV upon protein binding was observed (Figure 4). This shift is similar in magnitude to shifts observed upon addition of protein to ferrocene−peptide conjugates attached to a monolayer.[8,20] From this study, it was determined that the C11 hydroxyalkanethiol, shorter than the C16 alkanethiol ligand of the cluster, lessens the steric hindrance of protein binding at the surface of the monolayer, as this architecture results in larger observable electrochemical shifts upon protein binding. As in solution, the shift to more negative

dx.doi.org/10.1021/la202882k |*Langmuir* 2012, 28, 939–949

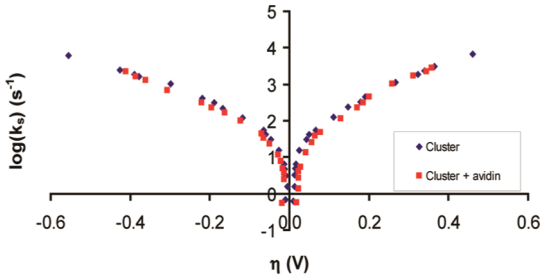

Figure 5. Tafel plot of electrochemistry of **9** before (blue diamonds) and after (red squares) 30 μM avidin soak overnight at 37 °C. Upon avidin addition, no observable change in the *y*-intercept (k_0) and curvature (λ) was observed.

potentials upon avidin addition is indicative of the oxidized form of the cluster becoming more stable in the environment of avidin.[6]

To show that the shift in $E_{1/2}$ was due to protein binding, a control system was employed in which a monolayer was formed using 20:1 diluent/cluster, where the diluent was HO-$(CH_2)_{11}$SH and the cluster was **10**. Since the bis-pyridine cluster does not contain an avidin binding ligand, no avidin binding should occur. After submerging the monolayer in a solution of 30 μM avidin at 37 °C overnight to maximize any potential protein interactions with the cluster or the monolayer, cyclic voltammetry was performed. No change in $E_{1/2}$ was observed, indicating that the binding of avidin to the cluster was the cause for the observed shift using **9** (SI Figure S12). However, in the voltammogram it can be seen that there is some decrease in current after avidin addition. The likely cause for this decrease in current is nonspecific binding of avidin to the monolayer. Further evidence that nonspecific binding is the cause of this current decrease is the lack of a decrease in current after incubation of a monolayer containing **10** in H_2O at 37 °C overnight (see SI Figure S13). As has been observed for other protein-based electrochemical systems, addition of protein decreases the observed faradaic current relative to the case where no protein is present.[13,85,86]

The explanation for this phenomenon is that the protein on the surface of the monolayer blocks free diffusion of the counterions to and from the redox species.[85] Since it is more difficult for counterions to diffuse to the redox center to balance the charge, electron transfer is hindered and a decrease in current is observed. To minimize nonspecific interactions, future studies will utilize poly(ethylene glycol) (PEG) terminated diluent alkanethiols. PEG terminated diluents have previously been shown to prevent nonspecific binding of protein to monolayer surfaces.[87] These experiments provide additional evidence that nonspecific protein binding confounds biosensors that are based on detecting decreases in current. Biosensors that rely on a change in redox potential are therefore advantageous over those that rely on negative feedback.

Electron Transfer Parameters. Using Laviron analysis of generated Tafel plots for the C16 diluent system, the rate of electron transfer was observed to be approximately 0.5 s^{-1} (SI Figures S7−S10).[4] This value is similar to previously reported literature values of 1 s^{-1} for comparable systems.[80,88,89] For the C11 diluent system, based on analysis of Tafel plots, the rate of electron transfer was observed to be approximately 75 s^{-1} (Figure 5). This value is an intermediate between literature values reported for a C16 system and a C11 system (1000 s^{-1}).[80,88] This intermediate value is believed to be due, in part, to through-space electron transfer between the cluster-alkanethiol and adjacent diluent alkanethiols. The C16 linker is flexible enough to allow the cluster to reach the shorter C11 diluent, providing a shorter tunneling pathway to the electrode. The through-space component to this mechanism results in a rate slower than that observed for a C11 system but faster than that observed for a C16 system.

Table 5. Monolayer Electrochemical Data before and after Avidin Binding for Monolayers Formed Using a Ratio of 20:1 Diluent $HO(CH_2)_{11}SH$ to Cluster[a]

compound	$E_{1/2}$ (mV)	$E_{1/2}$ with avidin (mV)	$\Delta E_{1/2}$ (mV)	k_{ET} (s^{-1})
$[Ru_3O(OAc)_6(4\text{-BMP})(py)(pyC16SH)]^+$	−46	−52	−6	60
$[Ru_3O(OAc)_6(4\text{-BMP})_2(pyC16SH)]^+$	−65	−108	−43	75
$[Ru_3O(OAc)_6(py)_2(pyC16SH)]^+$	−76	−76	0	60

[a] Potentials are reported vs Ag/AgCl.

Despite changes in $E_{1/2}$ upon avidin addition to the monolayer, Tafel plot analysis using the Laviron method showed no observable changes in both the rate of electron transfer (k_{ET}) and the reorganization energy (λ) for **9** (Figure 5).[4,90] The Tafel plots of the monolayer, before and after protein binding, overlay each other. There was no discernible change in curvature and the *y*-intercept of the graph, which indicates no measurable change in λ and k_{ET}, respectively.[4] A possible reason for an unobservable change in λ and k_{ET} in the cluster-based system is the metal-centered nature of the +1/0 redox reaction for the trinuclear ruthenium cluster system.[91] The electrons are delocalized only on the metal cluster. Delocalization does not extend to the binding ligands. Since there is lack of electron density on the binding ligands of the cluster, protein binding is less likely to affect λ and k_{ET} of the electron transfer process than in a system where electron density is delocalized to the binding ligands.

We hypothesize that the observed shift in $E_{1/2}$ upon protein binding to **9** is due more to a change in the Gibbs free energy associated with the electron transfer process than to a change in reorganization energy. The shift to more negative potentials upon avidin addition is indicative of the oxidized form of the cluster becoming more stable in the environment of avidin. Modeling showed that the ruthenium cluster portion of these complexes is near a hydrophilic portion of avidin, making the neutral, reduced state less stable.

Using the optimized diluent/cluster ratio and composition for monolayer formation as determined for **9**, monolayers were formed with 20:1 diluent/cluster where the diluent was HO-$(CH_2)_{11}$SH and the cluster was the monovalent complex, **8**. Cyclic voltammetry was performed for a series of scan rates, and Tafel plot analysis was performed. Values for $E_{1/2}$ and k_{ET} were similar to those observed for **9** (Table 5). As was observed previously, no observable change was observed in electron transfer rate and reorganization energy upon avidin addition. However, unlike the bivalent system, only small changes were observed for $E_{1/2}$ upon avidin binding (SI Figure S14). If intramolecular protein binding is occurring for the bivalent monolayer system, **9** would be more buried in the protein than **8** would be with its monovalent interaction, resulting in larger changes in $E_{1/2}$ upon protein binding. This result suggests that the bivalent interaction of **9** has a positive impact on the sensitivity of the monolayer system as compared to the monovalent interaction of **8**.

dx.doi.org/10.1021/la202882k |*Langmuir* 2012, 28, 939–949

CONCLUSIONS

Several biotinylated trinuclear ruthenium clusters were synthesized to test the effect of monovalent vs bivalent interactions on protein binding and electron transfer rates of surface-modified monolayers. Using HABA/avidin assays, **3** and **4** were shown to bind to avidin. Binding constants as measured by ITC were found to be $(6.5-8.0) \times 10^6\ M^{-1}$. Native gel electrophoresis showed an intermolecular binding mechanism in solution for **4**. This binding mode is the likely cause for the similar shifts in $E_{1/2}$ observed for **3** and **4** upon avidin addition. The size of the cluster allowed electronic coupling with the electrode to be maintained after protein binding, lessening the insulating effect of the protein experienced by small metal complexes in solution upon protein binding. Modeling studies indicated that it is possible for intramolecular binding to occur when intermolecular binding is inhibited. Clusters were synthesized with alkanethiols for the formation of self-assembled monolayers, facilitating detailed electrochemical analysis. For surface-bound clusters, optimization of diluent/cluster ratio and composition was necessary to obtain maximum protein binding. Negligible change in $E_{1/2}$ was observed after avidin addition to **8** and **10**. A change in $E_{1/2}$ of −43 mV was observed after avidin addition to **9** showing that the bivalent interaction has a positive impact on sensitivity to protein binding for the monolayer system. Future work will focus on modifications to the cluster system, tuning electron transfer parameters to further enhance electrochemical changes upon protein binding. These new probes will be explored as sensitive electrochemical protein biosensors.

ASSOCIATED CONTENT

Supporting Information. Experimental procedures for syntheses of **1**−**7** and the HABA/avidin assays. ITC data for 4-BMP, **3**, and **4**. Cyclic voltammetric data for **3a**, **8**, **9** (and for different cluster concentrations of **9** in the monolayer), and **10**. Native gel containing native avidin, **3**, and **4**. Energy vs time plot showing the equilibrium condition at 5 ns of **4** bound to avidin. This material is available free of charge via the Internet at http://pubs.acs.org.

AUTHOR INFORMATION

Corresponding Author

*E-mail: a-eckermann@northwestern.edu, tmeade@northwestern.edu.

ACKNOWLEDGMENT

The authors would like to thank Professor Clifford Kubiak, Dr. Kylie Barker, and Dr. Renee Strauch for helpful discussions. NMR spectroscopy was performed in the Northwestern University Integrated Molecular Structure and Research Center (IMSERC); full funding disclosure can be found at http://pyrite.chem.northwestern.edu. ITC was performed in the Keck Biophysics Facility at Northwestern University. Molecular modeling and computational chemistry services were provided by the Center for Molecular Innovation and Drug Discovery (CMIDD) at Northwestern University, which is funded by the Chicago Biomedical Consortium with support from The Searle Funds at The Chicago Community Trust. This research was supported by the National Institutes of Health under Award No. R01EB005866, the National Cancer Institute Center for Cancer Nanotechnology Excellence initiative at Northwestern University Award No. U54CA119341, the Chemistry of Life Processes Institute Lambert Fellows Program at Northwestern University, and by Ohmx Corporation.

REFERENCES

(1) Cheng, A. K. H.; Sen, D.; Yu, H.-Z. *Bioelectrochemistry* **2009**, *77* (1), 1–12.
(2) Ahrens, M. J.; Bertin, P. A.; Gaustad, A. G.; Georganopoulou, D.; Wunder, M.; Blackburn, G. F.; Gray, H. B.; Meade, T. J. *Dalton Trans.* **2011**, *40* (8), 1732–1736.
(3) Martic, S.; Labib, M.; Kraatz, H.-B. *Analyst* **2011**, *136* (1), 107–112.
(4) Eckermann, A. L.; Feld, D. J.; Shaw, J. A.; Meade, T. J. *Coord. Chem. Rev.* **2010**, *254* (15−16), 1769–1802.
(5) Bertin, P. A.; Meade, T. J. *Tetrahedron Lett.* **2009**, *50* (38), 5409–5412.
(6) Barker, K. D.; Eckermann, A. L.; Sazinsky, M. H.; Hartings, M. R.; Abajian, C.; Georganopoulou, D.; Ratner, M. A.; Rosenzweig, A. C.; Meade, T. J. *Bioconjugate Chem.* **2009**, *20* (10), 1930–1939.
(7) Tharamani, C. N.; Mahmoud, K. A.; Vasanthakumar, G. R.; Kraatz, H.-B. *Sens. Actuators, B: Chem.* **2009**, *B137* (1), 253–258.
(8) Kerman, K.; Kraatz, H.-B. *Analyst* **2009**, *134* (12), 2400–2404.
(9) Bertin, P. A.; Georganopoulou, D.; Liang, T.; Eckermann, A. L.; Wunder, M.; Ahrens, M. J.; Blackburn, G. F.; Meade, T. J. *Langmuir* **2008**, *24* (16), 9096–9101.
(10) Song, H.; Kerman, K.; Kraatz, H.-B. *Chem. Commun.* **2008**, *4*, 502–504.
(11) Kerman, K.; Song, H.; Duncan, J. S.; Litchfield, D. W.; Kraatz, H.-B. *Anal. Chem.* **2008**, *80* (24), 9395–9401.
(12) Kerman, K.; Mahmoud, K. A.; Kraatz, H.-B. *Chem. Commun.* **2007**, *37*, 3829–3831.
(13) Eckermann, A. L.; Barker, K. D.; Hartings, M. R.; Ratner, M. A.; Meade, T. J. *J. Am. Chem. Soc.* **2005**, *127* (34), 11880–11881.
(14) Umek, R. M.; Lin, S. W.; Vielmetter, J.; Terbrueggen, R. H.; Irvine, B.; Yu, C. J.; Kayyem, J. F.; Yowanto, H.; Blackburn, G. F.; Farkas, D. H.; Chen, Y.-P. *J. Mol. Diagnostics* **2001**, *3* (2), 74–84.
(15) Sadik, O. A.; Mwilu, S. K.; Aluoch, A. *Electrochim. Acta* **2010**, *55* (14), 4287–4295.
(16) Daniels, J. S.; Pourmand, N. *Electroanalysis* **2007**, *19* (12), 1239–1257.
(17) Cash, K. J.; Ricci, F.; Plaxco, K. W. *J. Am. Chem. Soc.* **2009**, *131* (20), 6955–6957.
(18) Das, J.; Kelley, S. O. *Anal. Chem.* **2011**, *83* (4), 1167–1172.
(19) Ishikawa, F. N.; Chang, H.-K.; Curreli, M.; Liao, H.-I.; Olson, C. A.; Chen, P.-C.; Zhang, R.; Roberts, R. W.; Sun, R.; Cote, R. J.; Thompson, M. E.; Zhou, C. *ACS Nano* **2009**, *3* (5), 1219–1224.
(20) Mahmoud, K. A.; Kraatz, H.-B. *Chem.—Eur. J.* **2007**, *13* (20), 5885–5895.
(21) Papp, I.; Sieben, C.; Ludwig, K.; Roskamp, M.; Boettcher, C.; Schlecht, S.; Herrmann, A.; Haag, R. *Small* **2010**, *6* (24), 2900–2906.
(22) Kluza, E.; van der Schaft, D. W. J.; Hautvast, P. A. I.; Mulder, W. J. M.; Mayo, K. H.; Griffioen, A. W.; Strijkers, G. J.; Nicolay, K. *Nano Lett.* **2010**, *10* (1), 52–58.
(23) Casas-Solvas, J. M.; Ortiz-Salmeron, E.; Garcia-Fuentes, L.; Vargas-Berenguel, A. *Org. Biomol. Chem.* **2008**, *6* (22), 4230–4235.
(24) Green, N. M. *Adv. Protein Chem.* **1975**, *29*, 85–133.
(25) Green, N. M. *Methods Enzymol.* **1990**, *184*, 51–67.
(26) Sugawara, K.; Tanaka, S.; Nakamura, H. *Anal. Chem.* **1995**, *67* (2), 299–302.
(27) Anzai, J.; Hoshi, T.; Osa, T. *Chem. Lett.* **1993**, *7*, 1231–1234.
(28) Pantano, P.; Kuhr, W. G. *Anal. Chem.* **1993**, *65* (5), 623–630.
(29) Livnah, O.; Bayer, E. A.; Wilchek, M.; Sussman, J. L. *Proc. Natl. Acad. Sci.* **1993**, *90* (11), 5076–5080.
(30) Weber, P. C.; Pantoliano, M. W.; Thompson, L. D. *Biochemistry* **1992**, *31* (39), 9350–9354.
(31) Livnah, O.; Sussman, J. L. *Methods Enzymol.* **1990**, *184*, 90−93.

(32) Toma, S. H.; Santos, J. J.; Araki, K.; Toma, H. E. *Eur. J. Inorg. Chem.* **2011**, *10*, 1640–1648.
(33) Glover, S. D.; Goeltz, J. C.; Lear, B. J.; Kubiak, C. P. *Coord. Chem. Rev.* **2010**, *254* (3−4), 331–345.
(34) Glover, S. D.; Goeltz, J. C.; Lear, B. J.; Kubiak, C. P. *Eur. J. Inorg. Chem.* **2009**, *5*, 585–594.
(35) Lear, B. J.; Glover, S. D.; Salsman, J. C.; Londergan, C. H.; Kubiak, C. P. *J. Am. Chem. Soc.* **2007**, *129* (42), 12772–12779.
(36) Salsman, J. C.; Ronco, S.; Londergan, C. H.; Kubiak, C. P. *Inorg. Chem.* **2006**, *45* (2), 547–554.
(37) Londergan, C. H.; Salsman, J. C.; Lear, B. J.; Kubiak, C. P. *Chem. Phys.* **2006**, *324* (1), 57–62.
(38) Lear, B. J.; Kubiak, C. P. *Inorg. Chem.* **2006**, *45* (18), 7041–7043.
(39) Londergan, C. H.; Kubiak, C. P. *J. Phys. Chem. A* **2003**, *107* (44), 9301–9311.
(40) Londergan, C. H.; Kubiak, C. P. *Chem.—Eur. J.* **2003**, *9* (24), 5962–5969.
(41) Londergan, C. H.; Salsman, J. C.; Ronco, S.; Dolkas, L. M.; Kubiak, C. P. *J. Am. Chem. Soc.* **2002**, *124* (22), 6236–6237.
(42) Ota, K.-i.; Sasaki, H.; Matsui, T.; Hamaguchi, T.; Yamaguchi, T.; Ito, T.; Kido, H.; Kubiak, C. P. *Inorg. Chem.* **1999**, *38* (18), 4070–4078.
(43) Ito, T.; Hamaguchi, T.; Nagino, H.; Yamaguchi, T.; Washington, J.; Kubiak, C. *Science* **1997**, *277* (5326), 660–663.
(44) Baumann, J. A.; Salmon, D. J.; Wilson, S. T.; Meyer, T. J.; Hatfield, W. E. *Inorg. Chem.* **1978**, *17* (12), 3342–3350.
(45) Uehara, H.; Inomata, T.; Abe, M.; Uosaki, K.; Sasaki, Y. *Chem. Lett.* **2008**, *37* (7), 684–685.
(46) Michi, T.; Abe, M.; Takakusagi, S.; Kato, M.; Uosaki, K.; Sasaki, Y. *Chem. Lett.* **2008**, *37* (6), 576–577.
(47) Abe, M.; Michi, T.; Sato, A.; Kondo, T.; Zhou, W.; Ye, S.; Uosaki, K.; Sasaki, Y. *Angew. Chem., Int. Ed.* **2003**, *42* (25), 2912–2915.
(48) Gallagher, S. R. One-Dimensional Electrophoresis Using Nondenaturing Conditions. In *Current Protocols in Molecular Biology*; John Wiley & Sons, Inc.: New York, 1999; pp 10.2B.1−10.2B.11.
(49) Zhou, W.; Zhang, Y.; Abe, M.; Uosaki, K.; Osawa, M.; Sasaki, Y.; Ye, S. *Langmuir* **2008**, *24* (15), 8027–8035.
(50) Abe, M.; Sasaki, Y.; Yamada, Y.; Tsukahara, K.; Yano, S.; Yamaguchi, T.; Tominaga, M.; Taniguchi, I.; Ito, T. *Inorg. Chem.* **1996**, *35* (23), 6724–6734.
(51) *Jaguar 7.7*; Schrödinger, LLC: New York, 2010.
(52) Becke, A. D. *J. Chem. Phys.* **1993**, *98* (7), 5648–5652.
(53) Lee, C.; Yang, W.; Parr, R. G. *Phys. Rev. B* **1988**, *37* (2), 785–789.
(54) Brandt, P.; Norrby, T.; Aakermark, B.; Norrby, P.-O. *Inorg. Chem.* **1998**, *37* (16), 4120–4127.
(55) Hay, P. J.; Wadt, W. R. *J. Chem. Phys.* **1985**, *82* (1), 299–310.
(56) Allinger, N. L.; Zhou, X.; Bergsma, J. *THEOCHEM* **1994**, *118* (1), 69–83.
(57) Norrby, P.-O.; Liljefors, T. *J. Comput. Chem.* **1998**, *19* (10), 1146–1166.
(58) Pugliese, L.; Coda, A.; Malcovati, M.; Bolognesi, M. *J. Mol. Biol.* **1993**, *231* (3), 698–710.
(59) *Sybyl-X 1.2*; Tripos International, 1699 Hanley Rd., St. Louis, Missouri, 63144, USA, 2010.
(60) *MacroModel 9.8*; Schrödinger, LLC: New York, 2010.
(61) Lo, K. K.-W.; Lau, J. S.-Y. *Inorg. Chem.* **2007**, *46* (3), 700–709.
(62) Green, N. M. *Methods Enzymol.* **1970**, *18* (Pt. A), 418–424.
(63) Green, N. M.; Konieczny, L.; Toms, E. J.; Valentine, R. C. *Biochem. J.* **1971**, *125* (3), 781–791.
(64) Green, N. M. *Biochem. J.* **1967**, *104* (3), 64P.
(65) Eisenberg-Domovich, Y.; Pazy, Y.; Nir, O.; Raboy, B.; Bayer, E. A.; Wilchek, M.; Livnah, O. *Proc. Natl. Acad. Sci.* **2004**, *101* (16), 5916–5921.
(66) D'Aquino, J. A.; Freire, E.; Amzel, L. M. *Proteins: Struct., Funct., Genetics* **2000**, No. Suppl. 4, 93–107.
(67) Lee, K. H.; Xie, D.; Freire, E.; Amzel, L. M. *Proteins: Struct., Funct., Genetics* **1994**, *20* (1), 68–84.
(68) Lo, K. K.-W.; Hui, W.-K. *Inorg. Chem.* **2005**, *44* (6), 1992–2002.
(69) Lo, K. K.-W.; Hui, W.-K.; Ng, D. C.-M. *J. Am. Chem. Soc.* **2002**, *124* (32), 9344–9345.
(70) Creus, M.; Pordea, A.; Rossel, T.; Sardo, A.; Letondor, C.; Ivanova, A.; LeTrong, I.; Stenkamp, R. E.; Ward, T. R. *Angew. Chem., Int. Ed.* **2008**, *47* (8), 1400–1404.
(71) Goeltz, J. C.; Hanson, C. J.; Kubiak, C. P. *Inorg. Chem.* **2009**, *48* (11), 4763–4767.
(72) Lear, B. J.; Kubiak, C. P. *J. Phys. Chem. B* **2007**, *111* (24), 6766–6771.
(73) Nunes, G. S.; Alexiou, A. D. P.; Araki, K.; Formiga, A. L. B.; Rocha, R. C.; Toma, H. E. *Eur. J. Inorg. Chem.* **2006**, *7*, 1487–1495.
(74) Hamaguchi, T.; Nagino, H.; Hoki, K.; Kido, H.; Yamaguchi, T.; Breedlove, B. K.; Ito, T. *Bull. Chem. Soc. Jpn.* **2005**, *78* (4), 591–598.
(75) Ito, T.; Imai, N.; Yamaguchi, T.; Hamaguchi, T.; Londergan, C. H.; Kubiak, C. P. *Angew. Chem., Int. Ed.* **2004**, *43* (11), 1376–1381.
(76) Toma, H. E.; Araki, K.; Alexiou, A. D. P.; Nikolaou, S.; Dovidauskas, S. *Coord. Chem. Rev.* **2001**, *219−221*, 187–234.
(77) Ito, T.; Hamaguchi, T.; Nagino, H.; Yamaguchi, T.; Kido, H.; Zavarine, I. S.; Richmond, T.; Washington, J.; Kubiak, C. P. *J. Am. Chem. Soc.* **1999**, *121* (19), 4625–4632.
(78) Baumann, J. A.; Wilson, S. T.; Salmon, D. J.; Hood, P. L.; Meyer, T. J. *J. Am. Chem. Soc.* **1979**, *101* (11), 2916–20.
(79) Bard, A. J.; Faulkner, L. R. *Electrochemical Methods: Fundamentals and Applications*, 2nd ed.; John Wiley & Sons, Inc.: New York, 2001; p 833.
(80) Eckermann, A. L.; Shaw, J. A.; Meade, T. J. *Langmuir* **2010**, *26* (4), 2904–2913.
(81) Bonanno, L. M.; DeLouise, L. A. *Langmuir* **2007**, *23* (10), 5817–5823.
(82) Jung, L. S.; Nelson, K. E.; Stayton, P. S.; Campbell, C. T. *Langmuir* **2000**, *16* (24), 9421–9432.
(83) Perez-Luna, V. H.; O'Brien, M. J.; Opperman, K. A.; Hampton, P. D.; Lopez, G. P.; Klumb, L. A.; Stayton, P. S. *J. Am. Chem. Soc.* **1999**, *121* (27), 6469–6478.
(84) Ren, C.-l.; Carvajal, D.; Shull, K. R.; Szleifer, I. *Langmuir* **2009**, *25* (20), 12283–12292.
(85) Sumner, J. J.; Creager, S. E. *J. Phys. Chem. B.* **2001**, *105* (37), 8739–8745.
(86) Mrksich, M.; Grunwell, J. R.; Whitesides, G. M. *J. Am. Chem. Soc.* **1995**, *117* (48), 12009–10.
(87) Jiang, X.; Bruzewicz, D. A.; Thant, M. M.; Whitesides, G. M. *Anal. Chem.* **2004**, *76* (20), 6116–6121.
(88) Haddox, R. M.; Finklea, H. O. *J. Phys. Chem. B* **2004**, *108* (5), 1694–1700.
(89) Chidsey, C. E. D. *Science* **1991**, *251* (4996), 919–922.
(90) Laviron, E. *J. Electroanal. Chem. Interfacial Electrochem.* **1979**, *101* (1), 19–28.
(91) Goeltz, J. C.; Benson, E. E.; Kubiak, C. P. *J. Phys. Chem. B* **2010**, *114* (45), 14729–14734.